



 Cite this: *RSC Adv.*, 2020, 10, 19952

Effect of polyvinylpyrrolidone (PVP) on palladium catalysts for direct synthesis of hydrogen peroxide from hydrogen and oxygen†

 Geun-Ho Han,^a Seok-Ho Lee,^a Myung-gi Seo^{*ab} and Kwan-Young Lee  ^{*ac}

When synthesizing nanoparticles in the liquid phase, polymeric materials (mainly polyvinylpyrrolidone, PVP) are applied as capping and/or stabilizing agents. The polymer layer on the nanoparticles must likely be removed since it blocks the active sites of the catalyst and inhibits mass transfer of the reactants. However, we have found that the polymer can have a positive effect on the direct synthesis of hydrogen peroxide. By testing Pd/SiO₂ catalysts with different amounts of PVP, it was revealed that an adequate amount of PVP resulted in a higher rate of hydrogen peroxide production (1001 mmol_{H₂O₂} g_{Pd}⁻¹ h⁻¹) than pristine Pd/SiO₂ did (750 mmol_{H₂O₂} g_{Pd}⁻¹ h⁻¹), unlike other PVP added Pd/SiO₂ catalysts containing excess PVP (less than 652 mmol_{H₂O₂} g_{Pd}⁻¹ h⁻¹). The effect of PVP on the catalysts was examined by transmission electron microscopy, Fourier transform infrared spectroscopy, CO chemisorption, thermogravimetric analysis, and X-ray photoelectron spectroscopy. For the catalysts containing PVP, the oxidation state of the palladium 3d shifted to high binding energy due to electron transfer from Pd to the PVP molecules. Consequently, the presence of PVP on the catalysts inhibited oxygen dissociation and decomposition of the produced hydrogen peroxide, resulting in a high selectivity and high production rate of hydrogen peroxide.

Received 8th April 2020

Accepted 18th May 2020

DOI: 10.1039/d0ra03148h

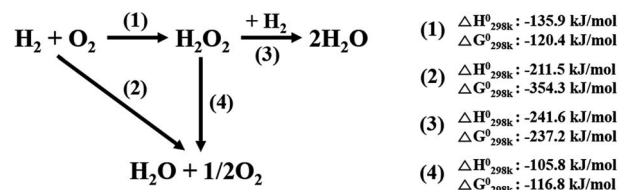
rsc.li/rsc-advances

Introduction

Hydrogen peroxide (H₂O₂) is used for numerous applications in global industries, including in the bleaching of pulp and paper, waste water treatment, semiconductor cleaning, soil remediation and the oxidization of chemical compounds.^{1,2} In particular, hydrogen peroxide is used to oxidize propene to produce value-added propylene oxide (Hydrogen Peroxide Propene Oxide, HPPO process). Commercially, hydrogen peroxide is manufactured by an auto-oxidation of anthraquinone which generates large amounts of harmful organic substances such as anthraquinone compounds.³ In addition, the commercial process requires substantial financial capital because it is separate redox processes involving complex multistage procedures. Moreover, it is only suitable for large-scale production, leading to difficulties associated with the transportation and storage of the produced hydrogen peroxide.⁴ To overcome these issues, there has been great research interest in developing

catalysts for the direct synthesis of hydrogen peroxide (DSHP) from hydrogen (H₂) and oxygen (O₂).⁵⁻¹⁰

The DSHP involves four primary reactions, as shown in Scheme 1. In addition to the desired reaction (1) that produces H₂O₂, three side reactions, namely, the formation of H₂O (2), the hydrogenation of H₂O₂ (3) and the decomposition of H₂O₂ (4), also occur. All the reactions are spontaneous due to their negative Gibbs free energies;¹¹ therefore, it is challenging to directly and selectively produce hydrogen peroxide. Additionally, the three-phase reaction system which results from the solid catalysts, liquid media, and gas reactants severely inhibits mass transfer of the reactants (H₂ and O₂). Hence, to overcome the hurdles that preclude the commercialization of the DSHP, the low yield of hydrogen peroxide should be solved by improving the conversion of reactants as well as the selectivity for hydrogen peroxide.



Scheme 1 Reaction pathways involved in the formation of hydrogen peroxide.

^aDepartment of Chemical and Biological Engineering, Korea University, 145 Anam-ro, Seoul 02841, Republic of Korea. E-mail: kylee@korea.ac.kr; Fax: +82-2-926-6102; Tel: +82-2-3290-3299

^bLotte Chemical, 115 Gajeongbuk-ro, Daejeon 34110, Republic of Korea. E-mail: bluebird677@gmail.com; Fax: +82-2-926-6102; Tel: +82-2-3290-3727

^cGraduate School of Energy and Environment (KU-KIST Green School), Korea University, Seoul 02841, Republic of Korea

† Electronic supplementary information (ESI) available. See DOI: 10.1039/d0ra03148h



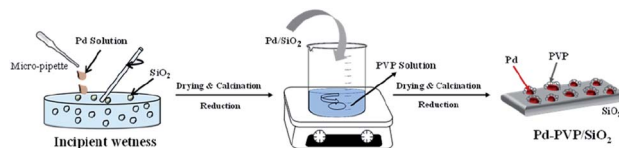
Recent studies have attempted to achieve this goal. In particular, computational chemistry^{12–14} and nanoparticle catalysts^{15–18} have been explored for improving the catalytic performance in the synthesis of hydrogen peroxide. In particular, a number of tailored structures and nanocatalysts with multiple metals have been developed. The exposed plane index of the metal nanoparticles (NPs) can be controlled based on the shape of the nanoparticles. The selectivity for hydrogen peroxide in the DSHP was improved by exposing only the (111) plane of Pd, as revealed by density functional theory (DFT) calculations by P. Tian *et al.*^{12,19} The effect of the size of the nanoparticles in the range of 3.5–20 nm was also examined. Our previous studies showed that smaller Pd nanoparticles showed lower hydrogen peroxide selectivity because the dangling bonds on the corner and edge sites of the nanoparticles facilitated O–O dissociation.^{20,21} In addition, bimetallic nanoparticles, including Pd–Pt, Pd–Au and Ag–Pt, offer improved yields of hydrogen peroxide, and reliable tools were applied to reveal their catalytic activities.^{16,17,22}

To synthesize the desired nanoparticles according to the aim, capping and/or stabilizing agents must be used.²³ Major function of stabilizing agents (*e.g.*, polyvinylpyrrolidone (PVP), and citric acid) can be summarized as follows: surface stabilizer, reducing agent, nanoparticle dispersant, and growth modifier.^{24–26} In a specific synthetic conditions, it stabilizes nanoparticles by enclosing their surfaces as well as provides individual space of nanoparticles by giving repulsive force. Such as PVP, surfactant can also act as a mild reducing agent for reduction metal salts. Moreover, preferable adsorption of surfactant on a specific facet of NPs induces facet controlled NPs like cubic, octahedral shape. Despite of those facile function of the surfactants, however, these agents on the surface of the nanoparticles could block the active sites and inhibit mass transfer of the reactants and products.¹¹ Thus, the elimination of these agents is generally required before the catalytic reaction.^{6,11} Nevertheless, complete removal of the surfactants under mild conditions that do not alter the tailored structure of the nanoparticles is exceedingly difficult. Hence, investigating the effects of stabilizing agents on the surface is of great importance because they interact with the active sites and can alter the electronic structure. Moreover, the discrepancy between the results obtained by DFT calculations and the catalytic tests of the nanoparticles can likely be narrowed. Herein, the effects of polyvinylpyrrolidone (PVP), the most common surfactant for NPs synthesis, on the catalytic properties of these systems were elucidated. Because it is difficult to control the removal of PVP from the as-synthesized Pd nanoparticles (or remove it completely), we added PVP to the Pd/SiO₂ catalyst. By varying the amount of adsorbed PVP on the Pd/SiO₂, we found that PVP had a positive effect on the DSHP.

Experimental

Chemicals

Polyvinylpyrrolidone (PVP, $M_w = 55\,000\text{ g mol}^{-1}$), palladium(II) nitrate dihydrate (Pd(NO₃)₂·2H₂O), ethanol (ACS reagent, $\geq 99.5\%$, absolute), silica gel (specific surface area = 480 m² g⁻¹,



Scheme 2 Two steps for preparing the Pd–PVP/SiO₂ catalyst.

pore volume = 0.75 cm³ g⁻¹), phosphoric acid (85 wt% in H₂O, $\geq 99.99\%$) and hydrogen peroxide (30 wt% in H₂O) were purchased from Sigma-Aldrich Co. All chemicals were used without further purification.

Catalyst synthesis

The PVP-containing Pd/SiO₂ catalyst was prepared in two steps as shown in Scheme 2. Since it is difficult to remove PVP from the synthesized nanoparticles, the catalyst was prepared according to the following steps: (i) preparation of the Pd/SiO₂ catalyst by the incipient wetness impregnation method and (ii) adsorption of the PVP by using PVP contained suspension. The details of the catalyst synthesis method are as follows.

A volume of Pd(NO₃)₂-containing solution corresponding to the pore volume of SiO₂ was impregnated into the SiO₂ by the incipient wetness method. The powder was dried overnight in an oven at 80 °C and then calcined at 500 °C for 3 h. Then, the prepared Pd/SiO₂ was reduced at 150 °C in a H₂ atmosphere to activate the oxidized Pd. After that, different amounts of PVP were added to 100 mL of deionized (DI) water to prepare aqueous suspensions containing 0.05 mM, 0.1 mM, and 0.2 mM of PVP. Subsequently, 2 g of the prepared Pd/SiO₂ was added to the PVP suspensions, and they were mixed at room temperature for 12 h. After mixing, the catalyst was obtained by filtration through filter paper, dried overnight in an oven at 80 °C, and then reduced in a H₂ atmosphere at 60 °C for 2 h. The synthesized catalysts were named Pd–PVP(1), Pd–PVP(2), and Pd–PVP(3), according to the concentration of the PVP suspension (0.05, 0.1, and 0.2 M, respectively).

Catalyst characterization

Transmission electron microscopy (TEM) was performed using a Tecnai G2 F30 transmission electron microscope (FEI Company, OR, USA) operating at 300 kV. The analysis was performed at the Korea Basic Science Institute (KBSI), Seoul. Scanning transmission electron microscopy (STEM) images were obtained by operating at 200 kV. Fourier transform infrared (FT-IR) spectroscopy (Perkin Elmer, Spectrum GX) was employed to study the adsorbed PVP in the catalysts. The spectra were recorded from 1300 to 2000 cm⁻¹ using 100 scans and a resolution of 4 cm⁻¹. The exposed specific area of Pd was determined *via* CO pulse chemisorption by using an ASAP 2020 chemisorption analyser (Micrometrics Inc., Norcross, USA). The Pd content of the catalyst was estimated by inductively coupled plasma optical emission spectrometry (ICP-OES) by using an iCAP-6300 duo ICP-OES spectrometer (Thermo Scientific, Waltham, MA, USA). The analysis was performed at the Korea Basic Science Institute (KBSI), Seoul. X-ray photoelectron



spectroscopy (XPS) analyses were used to measure the electronic states of N and Pd in each catalyst. XPS was performed using an ESCA2000 (VG Microtech, U.K.). Thermogravimetric analysis (TGA; TGA-N 1000, Scinco) was used to estimate the amount of PVP adsorbed on the catalysts. Prior to weight change measurement, the sample was heated to 150 °C under a N₂ flow of 50 mL min⁻¹ for removing water. Then, the sample was heated to 800 °C at a rate of 2 °C min⁻¹ under 50 mL min⁻¹ of air gas and the weight change was recorded.

Catalytic activity tests: direct synthesis of H₂O₂ from H₂ and O₂

H₂O₂ was directly synthesized using each catalyst in a double-jacket glass reactor. The reaction medium was composed of ethanol and water (150 mL, 20 vol% ethanol) containing 0.03 M of H₃PO₄. The reaction was performed at 10 °C and 1 bar with 1200 rpm stirring for 1 h, and the volumetric flow rate of the reactant gas stream (volume ratio of O₂/H₂ = 10) was 22 mL min⁻¹. The concentration of H₂O₂ in the solution was measured using iodometric titration after the reaction.²⁷ The H₂ concentration was measured *via* gas chromatography (Younglin, ACME6000 with a Carbosieve SII (60–80 mesh)) with a column and a thermal conductivity detector (TCD). Eqn (1)–(3) were used to calculate the H₂ conversion, H₂O₂ selectivity, and H₂O₂ production rate, respectively:

$$\text{H}_2 \text{ conversion}(\%) = \frac{\text{total moles of H}_2 \text{ reacted}}{\text{total moles of H}_2 \text{ fed}} \times 100 \quad (1)$$

$$\text{H}_2\text{O}_2 \text{ selectivity}(\%) = \frac{\text{moles of H}_2\text{O}_2 \text{ generated}}{\text{total moles of H}_2 \text{ reacted}} \times 100 \quad (2)$$

$$\begin{aligned} \text{H}_2\text{O}_2 \text{ production rate}(\text{mmol}_{\text{H}_2\text{O}_2} \text{ g}_{\text{Pd}}^{-1} \text{ h}^{-1}) \\ = \frac{\text{mmol of H}_2\text{O}_2 \text{ formed}}{\text{weight of Pd(g)in catalyst} \times \text{reaction time(h)}} \times 100 \quad (3) \end{aligned}$$

The H₂O₂ hydrogenation and decomposition tests were performed under the same reaction conditions, except that gas mixtures of H₂ + N₂ (22 mL min⁻¹, H₂/N₂ = 1/10, for hydrogenation) or pure N₂ (22 mL min⁻¹, for decomposition) were used instead of H₂ + O₂ feed. Then, 1 mL of 30% aqueous H₂O₂ solution was added. The concentration of remaining hydrogen peroxide was measured by the iodometric titration, and the fraction of converted H₂O₂ (%) was calculated with eqn (4) as follows.

$$\text{H}_2\text{O}_2 \text{ decomposition}(\%) = \frac{\text{initial concentration of H}_2\text{O}_2 - \text{final concentration of H}_2\text{O}_2}{\text{initial concentration of H}_2\text{O}_2} \times 100 \quad (4)$$

Safety

Using explosive gas feed composed of H₂ and O₂ should be controlled safely. Less than 4 mol% of H₂ with O₂ balance is an

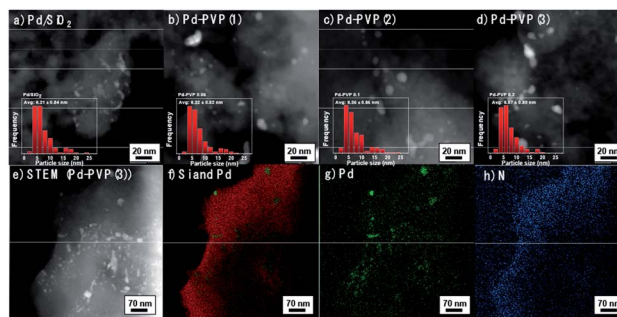


Fig. 1 STEM images for the catalysts (a–d). STEM image and EDS mapping images of Pd–PVP(3) catalyst. (e) STEM image, (f) EDS mapping image of Si and Pd element, (g) EDS mapping image of Pd element, and (h) EDS mapping image of N element.

out of explosive range. However, our research was performed under explosive range in order to obtain high H₂O₂ yield which is can be substantially affected by H₂/O₂ ratio. Under this explosive area, powder type catalyst should be banned. Instead, slurry phase catalyst including reaction medium with powder catalyst can avoid the explosion. In addition, high temperature catalyst powder can make a fire while it is mixed with the reaction medium, thus the slurry phase must be mixed with completely cooled powder.

Results and discussion

Prior to investigate the effect of PVP on Pd catalyst, several catalytic properties need to be controlled. In this perspective, size effect of Pd particles which has been reported in a number of researches should not be a main factor determining the catalytic activity.^{20,28,29} Thus, we prepared PVP added catalyst by using a pristine Pd/SiO₂ synthesized at once as described in the experimental section. Fig. 1a–d confirm that Pd particles, which appear in bright color, were dispersed on the surface of SiO₂ with negligible differences. They mainly present 5–7 nm size of Pd and some of agglomerated Pd particles co-existed. In terms of optimum size of Pd, F. Menegazzo and co-workers demonstrated Pd particle between 2–3 nm was able to activate O₂ molecules without dissociation, enabling selective H₂O₂ synthesis.³⁰ Meanwhile, P. Tian and co-workers found that sub-nano dominating (between 1.4–2.6 nm) Pd catalyst increased H₂O₂ selectivity, and especially, ~1.4 nm of Pd particles substantially improved the selectivity by suppressing H₂O pathway.³¹ On the other hand, under coordinate sites

denominated as corner or edge sites can be changed on the basis of particles size, which is crucial for H₂O₂ selectivity.^{20,29} More than 3.5 nm, the larger Pd particle exposed smaller ratio



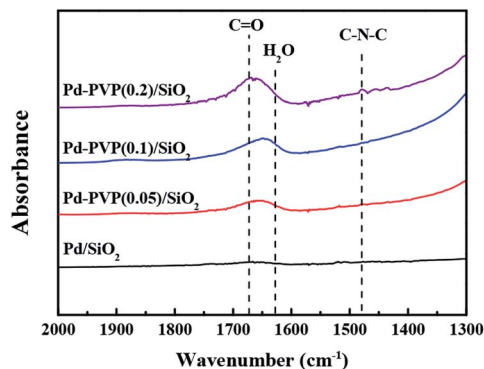


Fig. 2 Infrared spectra of the Pd/SiO₂, Pd-PVP(1), Pd-PVP(2), and Pd-PVP(3) catalysts.

of the under coordinate sites, resulting in high H₂O₂ selectivity. Based on the literatures, it can be said that the prepared Pd/SiO₂ and PVP-added Pd/SiO₂ catalysts are appropriate for investigating the effect of PVP addition due to their similar size distributions and size range over 3.5 nm (insets in Fig. 1a–d). In detail, the size distributions of the Pd particles were obtained by counting more than 150 number of particles and their average particles sizes were in the range of 6.07–6.35 nm.

In Fig. 2e–h, EDS mapping images for Pd-PVP(3) catalyst are shown to examine whether the PVP molecules adsorbed on the place we expected or not. Since nitrogen is a light element, unfortunately Pd-PVP(3) having enough amount of PVP molecules only exhibited reliable counts in the EDS analysis. As shown, bright color particles are in good agreement with Pd element points with green (Fig. 1e and g). However, it is found that N atoms are detected throughout the SiO₂, and more intense along with the surface of SiO₂, indicating PVP molecules distributed on the surface of SiO₂ without preference toward Pd particles. Thus, it can be supposed that Pd-PVP(3) contains excess amount of PVP.

Since the polymer, PVP, was difficult to be identified in the TEM images, the relative amount of PVP in the catalyst was confirmed by FT-IR analysis (Fig. 2). As shown, the characteristic peaks of the C=O and C–N–C bonds in PVP were observed at 1670 cm⁻¹ and 1480 cm⁻¹, respectively. When the higher concentration of PVP was used in preparation step, the C=O and C–N–C peaks were more intense as expected. The gradual

increase in the peak intensities indicated that larger amount of PVP was adsorbed on the Pd/SiO₂. In addition, Fig. 2 shows a shift of C=O bond from Pd-PVP(1) to Pd-PVP(3). It can be elucidated by the interaction between PVP and Pd particles. Through FT-IR spectra, pristine PVP and PVP interacting with metal particles can be determined by peak shift of carbonyl group (C=O).^{32,33} R. J. Kalbasi *et al.* reported that when carbonyl bond of PVP was coordinated to Pd particles, peak of C=O shifted to a lower wave number (1636 cm⁻¹) compared to the pristine PVP (1655 cm⁻¹).³² They suggested that the interaction between Pd and C=O bond resulted in weak CO stretches. Similarly, C.-L. Lee *et al.* compared PVP on Pd nanospheres with PVP molecule by FT-IR spectra.³³ They also found a shift of stretching frequency of the carbonyl group toward low wave number when PVP interacted with the Pd particles. Likewise, we also found a shift of carbonyl group over Pd-PVP(1) and Pd-PVP(2) compared to Pd-PVP(3), implying that PVP molecules in Pd-PVP(1) and Pd-PVP(2) properly formed interaction with Pd particles but Pd-PVP(3) included excess amount of PVP as supposed above TEM analysis.

In Table 1 and Fig. 3, the quantity of adsorbed PVP was measured by TGA analysis once more. The weight loss of the catalyst that is assigned to combustion of PVP molecule. In Fig. 3, solid lines indicate that Pd-PVP(1), (2), and (3) catalysts contained about 4, 7.5, and 10.8 wt% of PVP, respectively, before the DSHP reaction. However, unexpected continuous weight loss is observed in the temperature range over 400 °C.

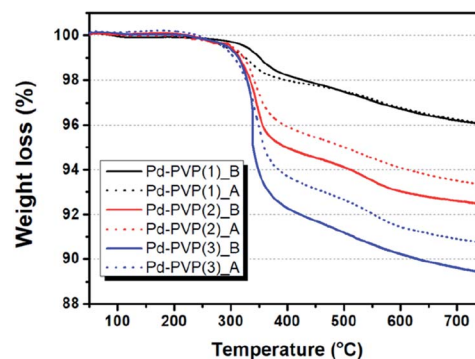


Fig. 3 TGA profiles of Pd-PVP(N) (N = 1, 2, and 3) catalysts before and after DSHP reaction. Denominated by 'B' indicates before reaction (solid line) and 'A' indicates after reaction (dotted line).

Table 1 Exposed Pd areas, peak centers of Pd 3d, and PVP loadings of the prepared catalysts

Catalyst	Exposed Pd area ^a (m ² g _{Pd} ⁻¹)	Peak center ^b (eV)		Actual PVP loading ^c (wt%)
		3d _{3/2}	3d _{5/2}	
Pd/SiO ₂	193	340.1	335.0	n.d.
Pd-PVP(1)	157	340.2	335.2	4.0
Pd-PVP(2)	133	340.2	335.2	7.5
Pd-PVP(3)	74	340.3	335.3	10.5

^a Exposed Pd areas were calculated by CO pulse chemisorption. ^b Peak centers of Pd 3d spectra were measured by XPS analysis. ^c Actual PVP loadings were measured by TGA analysis. n.d. indicates not determined.



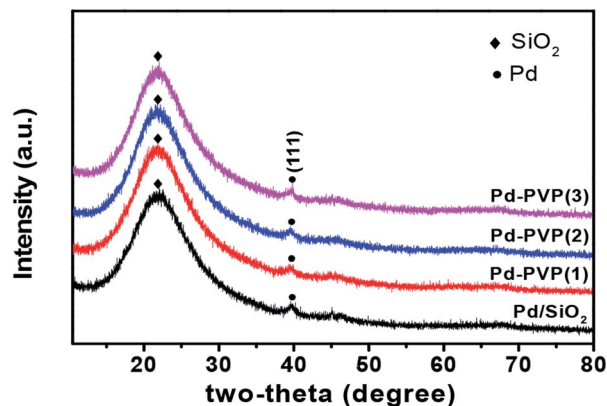


Fig. 4 XRD diffractogram of Pd/SiO₂ and Pd-PVP catalysts. Black circle indicates Pd(111) crystal plane and black diamond indicates amorphous SiO₂.

Since PVP combustion under air condition occurs mainly around 300–400 °C, it should be explained by other reason. The surface terminal groups of SiO₂, siloxane ($\equiv\text{Si}-\text{O}-\text{Si}\equiv$) and silanol ($\equiv\text{Si}-\text{OH}$), can be changed by thermal treatment. R. Mueller *et al.* determined that SiO₂ loses its surface hydroxyl group from 120 °C to 800 °C by using both TGA and titration analysis, resulting in continuous weight decrease.³⁴ According to this, we performed TG analysis for fresh Pd/SiO₂ without any PVP and presented it in Fig. S1.† First run of TGA for Pd/SiO₂ showed 0.8 wt% of continuous weight loss over 100 °C, corresponding to the literature. This weight loss didn't shown in second run of Pd/SiO₂, indicating that surface hydroxyl groups were completely eliminated during first run of TGA. Hence, exact weight loss of PVP in those catalysts could be re-calculated by subtracting weight loss of fresh Pd/SiO₂ (0.8 wt%), as follows: Pd-PVP(1) = 3.2 wt%, Pd-PVP(2) = 6.7 wt%, and Pd-PVP(3) = 10.0 wt%.

Interestingly, the weight loss of the catalysts are different after the reaction. When PVP molecules were contained more than 7.5 wt% (Pd-PVP(2) and (3)), the molecules were detached and/or decomposed of 1–1.5 wt% during the reaction. However, Pd-PVP(1) showed negligible difference in weight loss. Thus, it is notable to say that Pd-PVP(1) has an optimum amount of PVP for occurring the interaction between Pd and PVP, which cannot be defined in the IR spectra. In addition, the less weight loss of the used Pd-PVP(2) and (3) could be explained by detachment rather than decomposition, because, if it was decomposed, Pd-PVP(1) also showed a distinguishable weight loss after the reaction.

XRD data of the catalysts are shown at Fig. 4. A broad peak at 22° indicates amorphous SiO₂.³⁵ Palladium metal diffractogram are (JCPDS no. 46-1043 Pd) at 40°, 46°, and 68° which are assigned to Pd(111), Pd(200), Pd(220), respectively, but owing to low Pd content (~0.8 wt%), peaks of Pd(200) and Pd(220) are not distinct enough to be analyzed here, therefore only Pd(111) peak is identified and marked. However, it is obvious that metallic diffraction information of Pd is identified over all the catalysts, indicating that Pd catalyst was sufficiently activated to metallic state during reduction.

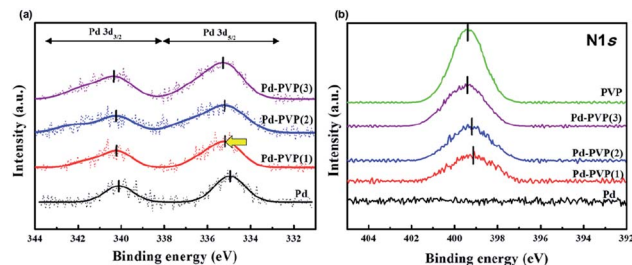


Fig. 5 XPS spectra of the catalysts. (a) Pd 3d region and (b) N 1s region of Pd/SiO₂, Pd-PVP(1), Pd-PVP(2), and Pd-PVP(3).

PVP can interact with the metal through either way; withdrawing electrons or providing electrons. In terms of the former, PVP molecules can interact with Pd particle due to their C=O and C–N–C bonds since those groups contain high electronegativity elements (*i.e.*, C, N, and O) compared to Pd. They can withdraw electron density from the electron-rich Pd particles to form the interaction. On the other hand, Y. Borodko *et al.* found that unshared electron pairs in O and N atoms provided themselves to electron deficient Pt, resulting in strong interaction between metal and PVP.³⁶ XPS analysis solved this uncertainty. In Fig. 5, the XPS spectra revealed how PVP and Pd exchanged electrons. The electronic state of Pd in the pristine Pd/SiO₂ was observed, and the signals of both Pd 3d_{5/2} and Pd 3d_{3/2} were almost equal to what is typical of metallic Pd⁰ (334.9 eV). However, the peak center in the spectra of the Pd-PVP/SiO₂ catalysts shifted to a higher binding energy (335.2–335.3 eV, Table 1). Moreover, the peak attributed to Pd²⁺ became more intense, meaning that PVP generated electron-deficient Pd species. In terms of the N 1s regions, the Pd-coordinated N 1s peaks shifted to a low binding energy (399.1 eV) compared to those of pristine PVP (399.4 eV). The N 1s peak was located at a lower binding energy when the catalyst contained a lower amount of PVP. This is because the exact amount of electron withdrawn by PVP molecules are similar, causing average electron state of N 1s gradually close to that of pristine PVP. It also is good agreement with the similar electronic state of Pd around at 335.2–335.3 eV of Pd-PVP catalysts even though they contain different amount of PVP. As a result, it is examined that electrons were transferred from the electron-rich Pd (induced by reduction step in preparation) to the nitrogen in PVP instead of forming interactions by the unshared electron pairs of nitrogen or oxygen atoms. In addition, notably, the electron transfer induced by PVP resulted in an electron-deficient Pd species, and especially, Pd-PVP(1) is an optimized catalyst in terms of PVP interacted Pd.

CO pulse chemisorption analysis was performed to measure the exposed Pd area as PVP content increased. As described above, since the amount of PVP in Pd-PVP(1) was enough to form interactions with Pd, decrease of the exposed Pd area (193 → 157 m² g_{Pd}⁻¹) can be derived by an occupation of Pd sites. Moreover, the exposed Pd area gradually decreased as the PVP content increased. It might be induced by PVP layers on the surface of Pd/SiO₂ which can crucially cause mass transfer



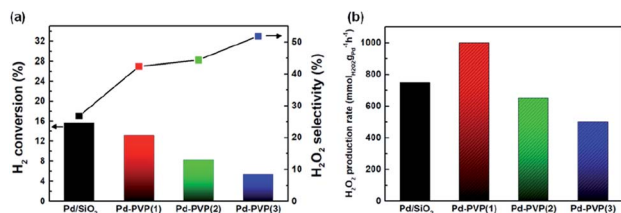


Fig. 6 Direct synthesis of hydrogen peroxide using Pd/SiO₂, Pd-PVP(1), Pd-PVP(2), and Pd-PVP(3) as catalysts in the presence of ethanol and H₃PO₄: (a) H₂ conversion and H₂O₂ selectivity; (b) H₂O₂ productivity (gram-Pd-specific H₂O₂ production rate).

limitation of gas molecules. Thus, for the catalytic activity, these situation is expected to reduce H₂ activation in DSHP reaction.

Fig. 6 shows the catalytic activity for DSHP with the prepared catalysts, including their H₂ conversions, H₂O₂ selectivities and H₂O₂ production rates. As the PVP content increased (Pd/SiO₂ → Pd-PVP(3)), the H₂ conversion decreased. This reduced H₂ conversion can be attributed to lowered amount of exposed Pd sites which mainly accounted for H₂ activation (Table 1). Based on the CO chemisorption results, larger PVP content resulted in lower Pd sites by either ways; interaction between Pd and PVP, and PVP polymer layer surrounding the Pd surface. For the latter, Giorgianni *et al.* investigated the effect of polyvinyl alcohol as a capping agent on the kinetics of direct hydrogen peroxide production.²⁸ The polyvinyl alcohol layers on the surface of the nanoparticle were shown to hinder mass transfer. Thus, in a similar manner, the PVP layers formed on the Pd likely impeded the mass transfer of the reactants. Therefore, removing PVP layers would be expected to enhance the catalytic activity as expected.

However, Pd-PVP(1)/SiO₂ achieved higher H₂O₂ production rate (1001 mmol_{H₂O₂}/g_{Pd} h⁻¹) than Pd/SiO₂ did (750 mmol_{H₂O₂}/g_{Pd} h⁻¹), which resulted from enhanced H₂O₂ selectivity of Pd-PVP(1) (Fig. 6b). Above characterizations for PVP added Pd/SiO₂ catalyst disclosed that the layers not only interrupted mass transfer but also influenced the oxidation state of Pd (Fig. 5). As described in the XPS analysis, overall, the Pd 3d region became more electron deficient when PVP was added.

The effect of the Pd oxidation state on the DSHP has been studied for explaining H₂O₂ selectivity. Choudhary *et al.* argued that unlike Pd⁰ (Pd metal), PdO (Pd²⁺) was a suitable catalyst for the selective synthesis of H₂O₂, because PdO inhibited the decomposition and hydrogenation of H₂O₂.^{37–39} N. M. Wilson *et al.* demonstrated that electron back-donation to adsorbed O–O molecules can facilitate O–O bond dissociation; thus, a lower electron density resulted in higher H₂O₂ selectivity.⁵ In terms of Pd-PVP catalyst, it was found by XPS analysis that PVP adsorbed Pd showed electron deficient state compared to pristine Pd/SiO₂. Correspondingly, as shown in Fig. 6, a comparison of the H₂O₂ selectivities of Pd-PVP(1) and Pd/SiO₂ suggested that the electron-deficient Pd in Pd-PVP(1) improved its H₂O₂ selectivity (27% → 42%) by suppressing O–O bond dissociation as well as further H₂O₂ decomposition. In addition, H₂O₂ selectivity continuously increased as PVP content increased (44% for Pd-PVP(2) and 52% for Pd-PVP(3)). However, it has to

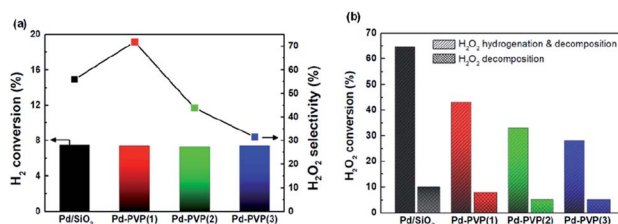


Fig. 7 (a) Iso-conversion DSHP results of the catalysts. It was obtained by varying the amount of Pd metal. (b) H₂O₂ hydrogenation and decomposition results of the catalysts. The H₂O₂ hydrogenation and decomposition tests were performed under (H₂ + N₂), and the decompositions tests were performed under pure N₂.

be pointed out here that a product (H₂O₂) selectivity of successive reaction such as DSHP can critically be affected by conversion of a reactant (H₂). For instance, one catalyst generally shows higher H₂O₂ selectivity at low H₂ conversion under different reaction conditions. Thus, to avoid a misunderstanding of H₂O₂ selectivity trend, H₂O₂ selectivity should be examined by iso-conversion tests as below.

Fig. 7a shows iso-conversion tests of the catalysts. By adjusting H₂ conversion to 7.5%, their H₂O₂ selectivity trend became more distinguishable and reliable. It was obvious that Pd-PVP(1) achieved the highest H₂O₂ selectivity of 72%. In addition, Pd-PVP(2) and Pd-PVP(3) having excess PVP showed gradual decrease in H₂O₂ selectivity. The reason for their low selectivity is proposed as the poor back-diffusion of the produced H₂O₂.²⁸ It was reported that poor back-diffusion caused by the layer of capping agent (polyvinyl alcohol) led to low H₂O₂ selectivity since further decomposition/hydrogenation of H₂O₂ to H₂O was unavoidable on the surface of catalyst. Thus, the excess PVP layers offset the positive effect of the PVP on electron-deficient Pd species, resulting in low H₂O₂ selectivity (72% → 32%).

Meanwhile, in terms of PVP molecule, its hydrophilicity/hydrophobicity can affect the catalytic performance. In detail, PVP has two main repeating group; pyrrolidone moiety (hydrophilic component) and alkyl group (considerable hydrophobic group).²⁴ Yao X. *et al.* measured octanol–water affinity coefficients (K_{AOW}) of nanoparticles with PVP to investigate hydrophobicity of the nanoparticles. K_{AOW} values higher than 1 mean a hydrophobic compound, while those less than 1 indicate a hydrophilic one. Over their NPs with PVP, K_{AOW} value of the NPs with PVP were close to 1, implying the amphiphilic property of PVP.⁴⁰ In addition, to stabilize metallic nanoparticles in aqueous solution, C=O bonds in PVP molecules surround the nanoparticles while pyrrolidone and alkyl group are placed outward,^{41,42} suggesting that the surface of Pd-PVP catalysts could expose either hydrophobic or hydrophilic groups. Thus, this study more focused on the distinct and observable effect of PVP on electronic alteration and mass transfer limitation.

Fig. 7b shows the results of the decomposition and hydrogenation of H₂O₂. The H₂O₂ decomposition rate and the hydrogenation rate of the catalysts gradually decreased as the



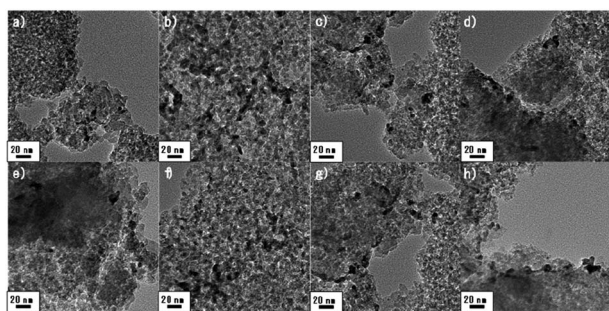


Fig. 8 TEM images of the catalysts before the DSHP; (a) Pd/SiO₂, (b) Pd-PVP(1), (c) Pd-PVP(2), and (d) Pd-PVP(3). TEM images of the catalysts after the reaction; (e) Pd/SiO₂, (f) Pd-PVP(1), (g) Pd-PVP(2), and (h) Pd-PVP(3).

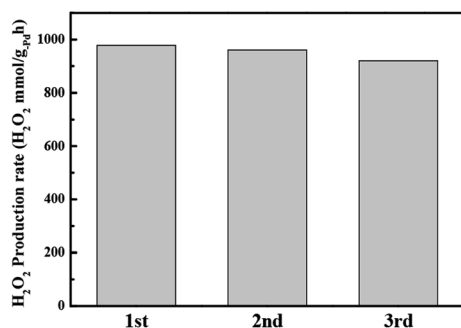


Fig. 9 Catalyst recycling test results (rate of H₂O₂ production by Pd-PVP(1)). Recycling tests were performed under the same conditions as the H₂O₂ direct synthesis tests.

PVP content increased. This phenomenon resulted from both alterations to the electronic state of Pd and mass transfer hindrance by PVP layer. By comparing the H₂O₂ conversions of Pd/SiO₂ and Pd-PVP(1), Pd-PVP(1) showed much higher order of lowered H₂O₂ conversion (64.5% and 43%, respectively) compared to H₂ conversion (15.7% and 13.2%, respectively). Suppression of the H₂O₂ conversion is well elucidated by the positive effect of electron deficient Pd species and also underpins the high H₂O₂ selectivity of Pd-PVP(1). Meanwhile, excess PVP suppressed the conversion of H₂O₂ to a great extent by hindering the mass transfer of the reactant from the bulk solution to the catalyst surface, which was in good agreement with the back-diffusion situation shown in Fig. 7a.

After the DSHP (Fig. 8), no distinguishable difference in the catalysts were observed, indicating that the textural properties of the Pd-PVP/SiO₂ catalysts were stable for DSHP reaction. However, the reuse test of the most active Pd-PVP(1) catalyst shows necessity of further study. As observed in Fig. 9, the activity of the catalyst slightly decreased when the catalyst was recycled accompanying slight increase of H₂ conversion (13.2 to 13.5%) and decrease of H₂O₂ selectivity (42% to 40%). From this result, it could be assume that there is an inevitable deactivation of PVP promotes catalyst despite of a loading of the adequate amount of PVP such as Pd-PVP(1). By using FT-IR spectra, a slight change of the peak intensity was observed. In Fig. S2,[†] those spectra of the pristine Pd-PVP(1) and 3rd used Pd-PVP(1) are shown in the range of PVP molecule bonds. Obvious C=O bond and C-N-C bond included in PVP molecule are observed in pristine Pd-PVP(1) catalyst, and the peak intensities of those bonds slightly decrease after the catalyst used. Considering the TGA data, Pd-PVP(1) can retain near most of adsorbed PVP but it can lose the molecules while repeating the DSHP reaction. Therefore, reusability of these catalysts needs to be further improved since PVP can be slightly but continuously detached from the surface of the catalyst during catalytic reactions.

To compare catalytic activities of Pd-PVP(1) with those of other developed catalysts, literatures were surveyed and summarized at below Table 2. It contains activity test results performed under similar reaction system (semi-batch and ambient pressure). It is observable that higher H₂O₂ selectivities were obtained with lower H₂ conversions although there are major unseen factors (*e.g.*, reaction temperature, feed ratio, medium, acid concentration, and electronic state of metals) determining the catalytic activity, especially over Pd mono-metal catalysts. Thus, by considering similar H₂ conversion, our PVP-modified Pd/SiO₂ (6.3 nm Pd) obtained comparable H₂O₂ selectivity to highly dispersed Pd catalyst such as Pd/N-TiO₂(c) (2.2 nm) and Pd/hydroxyapatite (1.6 nm), suggesting that those developed catalysts can be further improved by adopting our findings. In terms of bi-metal catalyst, Pd-Te showed 100% of H₂O₂ selectivity at low H₂ conversion of 6%, and a renowned Au-Pd catalysts showed 40% of H₂O₂ selectivity under no additive conditions, indicating that a great selectivity could be achieved with bi-metal modification. In a similar manner, those Pd based bimetal catalyst also has potential for being enhanced their activity through the surfactant effect.

Table 2 Catalytic activities for Pd/SiO₂ and Pd-PVP catalysts under different reduction conditions

Catalysts	Additives	H ₂ conv. (%)	H ₂ O ₂ selec. (%)	Ref.
Pd-PVP(1)	H ₃ PO ₄	7.5	72	This study
Pd/rutile TiO ₂	H ₃ PO ₄	9	56	43
Pd/N-TiO ₂ (c)	H ₂ SO ₄	6	75	44
Pd/hydroxyapatite	H ₂ SO ₄	2	94	31
Pd/mesoporous anatase TiO ₂	H ₂ SO ₄	40	40	45
Pd-tellurium/TiO ₂	H ₂ SO ₄	6	100	46
Au-Pd alloy	H ₂ SO ₄	None	59	47
Au-Pd alloy	None	32	40	48



Overall, the PVP in the synthesis of nanoparticles could play two roles. The highly electronegative nitrogen atoms in PVP can alter the electronic structure of the active sites by withdrawing electron density from the metal atoms. Additionally, when the concentration of PVP is sufficiently high, the PVP forms a surface layer that limits mass transfer of molecules. Thus, for Pd-PVP(1)/SiO₂, which has a suitable amount of PVP, the positive effect of PVP was dominant, resulting in the highest H₂O₂ selectivity and production rate. This study showed that the surfactants used in nanoparticle synthesis could alter the surface electronic states to being favourable for certain reactions. Hence, it is possible to both improve the catalytic activity and stabilize the nanoparticles by controlling the surface surfactant concentration rather than completely removing the surfactant.

Conclusions

We investigated the effects of PVP adsorbed on the catalyst surface in the DSHP by preparing PVP-adsorbed Pd/SiO₂ catalysts. The experimental results showed that the electrons of Pd migrated to the PVP, inducing the electron deficient Pd species for high H₂O₂ selectivity. Excess PVP on the Pd surface was shown to inhibit the mass transfer of the reactants and impede the production of hydrogen peroxide. The former caused low H₂ conversion, and the latter caused low H₂O₂ selectivity due to further decomposition. In conclusion, an adequate amount of PVP on the Pd/SiO₂ catalyst improved the H₂O₂ selectivity compared to slight decrease in H₂ conversion, leading to the highest H₂O₂ production rate of 1001 mmol_{H₂O₂} g_{Pd}⁻¹ h⁻¹. From this study, it is notably found that moderate content of such surfactants on the particle surface provide a betterment compared to a complete elimination of them. In addition, stable interaction between N containing groups and Pd can be considered as a promising way to develop DSHP-adequate catalysts in terms of electron deficient +Pd species.

Conflicts of interest

There are no conflicts to declare.

Acknowledgements

This work was supported by the National Research Foundation of Korea (NRF) grant funded by the Korean government (MSIP) (NRF-2016M3D1A1021143).

Notes and references

- 1 M. Ksibi, *Chem. Eng. J.*, 2006, **119**, 161–165.
- 2 X. S. Chai, Q. X. Hou, Q. Luo and J. Y. Zhu, *Anal. Chim. Acta*, 2004, **507**, 281–284.
- 3 N. Mizuno, *Modern Heterogeneous Oxidation Catalysis*, Wiley-VCH, 2009.
- 4 J. M. Campos-Martin, G. Blanco-Brieva and J. L. G. Fierro, *Angew. Chem., Int. Ed.*, 2006, **45**, 6962–6984.
- 5 N. M. Wilson and D. W. Flaherty, *J. Am. Chem. Soc.*, 2016, **138**, 574–586.
- 6 M.-g. Seo, D.-W. Lee, S. S. Han and K.-Y. Lee, *ACS Catal.*, 2017, **7**, 3039–3048.
- 7 G.-H. Han, M.-g. Seo, Y.-H. Cho, S. S. Han and K.-Y. Lee, *Mol. Catal.*, 2017, **429**, 43–50.
- 8 S. J. Freakley, Q. He, J. H. Harrhy, L. Lu, D. A. Crole, D. J. Morgan, E. N. Ntainjua, J. K. Edwards, A. F. Carley, A. Y. Borisevich, C. J. Kiely and G. J. Hutchings, *Science*, 2016, **351**, 965–968.
- 9 X. Xiao, T.-U. Kang, H. Nam, S. H. Bhang, S. Y. Lee, J.-P. Ahn and T. Yu, *Korean J. Chem. Eng.*, 2018, **35**, 2379–2383.
- 10 Y. Jang, H. Nam, J. Song, S. Lee, J.-P. Ahn and T. Yu, *Korean J. Chem. Eng.*, 2019, **36**, 1417–1420.
- 11 M.-g. Seo, H. J. Kim, S. S. Han and K.-Y. Lee, *Catal. Surv. Asia*, 2017, **21**, 1–12.
- 12 P. Tian, L. Ouyang, X. Xu, J. Xu and Y.-F. Han, *Chin. J. Catal.*, 2013, **34**, 1002–1012.
- 13 T. Deguchi and M. Iwamoto, *J. Phys. Chem. C*, 2013, **117**, 18540–18548.
- 14 A. Staykov, T. Kamachi, T. Ishihara and K. Yoshizawa, *J. Phys. Chem. C*, 2008, **112**, 19501–19505.
- 15 H. E. Jeong, S. Kim, M.-g. Seo, D.-W. Lee and K.-Y. Lee, *J. Mol. Catal. A: Chem.*, 2016, **420**, 88–95.
- 16 S. Quon, D. Y. Jo, G.-H. Han, S. S. Han, M.-g. Seo and K.-Y. Lee, *J. Catal.*, 2018, **368**, 237–247.
- 17 I. Kim, M.-g. Seo, C. Choi, J. S. Kim, E. Jung, G.-H. Han, J.-C. Lee, S. S. Han, J.-P. Ahn, Y. Jung, K.-Y. Lee and T. Yu, *ACS Appl. Mater. Interfaces*, 2018, **10**, 38109–38116.
- 18 A. Villa, S. Freakley, M. Schiavoni, J. K. Edwards, C. Hammond, G. M. Veith, W. Wang, D. Wang, L. Prati and N. Dimitratos, *Catal. Sci. Technol.*, 2016, **6**, 694–697.
- 19 S. Kim, D.-W. Lee and K.-Y. Lee, *J. Mol. Catal. A: Chem.*, 2014, **391**, 48–54.
- 20 S. Kim, D.-W. Lee, K.-Y. Lee and E. A. Cho, *Catal. Lett.*, 2014, **144**, 905–911.
- 21 H. E. Jeong, S. Kim, M.-g. Seo, D.-W. Lee and K.-Y. Lee, *J. Mol. Catal. A: Chem.*, 2016, **420**, 88–95.
- 22 N. M. Wilson, Y.-T. Pan, Y.-T. Shao, J.-M. Zuo, H. Yang and D. W. Flaherty, *ACS Catal.*, 2018, **8**, 2880–2889.
- 23 M. Jin, H. Zhang, Z. Xie and Y. Xia, *Energy Environ. Sci.*, 2012, **5**, 6352–6357.
- 24 K. M. Koczkur, S. Mourdikoudis, L. Polavarapu and S. E. Skrabalak, *Dalton Trans.*, 2015, **44**, 17883–17905.
- 25 D. J. Bharali, S. K. Sahoo, S. Mozumdar and A. Maitra, *J. Colloid Interface Sci.*, 2003, **258**, 415–423.
- 26 S.-D. Oh, B.-K. So, S.-H. Choi, A. Gopalan, K.-P. Lee, K. R. Yoon and I. S. Choi, *Mater. Lett.*, 2005, **59**, 1121–1124.
- 27 H. Lee, S. Kim, D.-W. Lee and K.-Y. Lee, *Catal. Commun.*, 2011, **12**, 968–971.
- 28 G. Giorgianni, S. Abate, G. Centi and S. Perathoner, *ChemCatChem*, 2019, **11**(1), 550–559.
- 29 P. Tian, D. Ding, Y. Sun, F. Xuan, X. Xu, J. Xu and Y.-F. Han, *J. Catal.*, 2019, **369**, 95–104.
- 30 F. Menegazzo, M. Signoretto, G. Frison, F. Pinna, G. Strukul, M. Manzoli and F. Boccuzzi, *J. Catal.*, 2012, **290**, 143–150.



- 31 P. Tian, L. Ouyang, X. Xu, C. Ao, X. Xu, R. Si, X. Shen, M. Lin, J. Xu and Y.-F. Han, *J. Catal.*, 2017, **349**, 30–40.
- 32 R. J. Kalbasi and N. Mosaddegh, *Mater. Chem. Phys.*, 2011, **130**, 1287–1293.
- 33 C.-L. Lee, R.-B. Wu and C.-M. Syu, *Electrochem. Commun.*, 2009, **11**, 270–273.
- 34 R. Mueller, H. K. Kammler, K. Wegner and S. E. Pratsinis, *Langmuir*, 2003, **19**, 160–165.
- 35 Y. Liang, J. Ouyang, H. Wang, W. Wang, P. Chui and K. Sun, *Appl. Surf. Sci.*, 2012, **258**, 3689–3694.
- 36 Y. Borodko, S. M. Humphrey, T. D. Tilley, H. Frei and G. A. Somorjai, *J. Phys. Chem. C*, 2007, **111**, 6288–6295.
- 37 V. R. Choudhary, A. G. Gaikwad and S. D. Sansare, *Catal. Lett.*, 2002, **83**, 235–239.
- 38 V. R. Choudhary, S. D. Sansare and A. G. Gaikwad, *Catal. Lett.*, 2002, **84**, 81–87.
- 39 A. G. Gaikwad, S. D. Sansare and V. R. Choudhary, *J. Mol. Catal. A: Chem.*, 2002, **181**, 143–149.
- 40 Y. Xiao and M. R. Wiesner, *J. Hazard. Mater.*, 2012, **215**, 146–151.
- 41 M. Behera and S. Ram, *Appl. Nanosci.*, 2013, **3**, 543–548.
- 42 A.-Q. Zhang, L.-J. Cai, L. Sui, D.-J. Qian and M. Chen, *Polym. Rev.*, 2013, **53**, 240–276.
- 43 G.-H. Han, G. P. Lee and K.-Y. Lee, *Catal. Today*, 2019, **352**, 262–269.
- 44 C. Ao, P. Tian, L. Ouyang, G. Da, X. Xu, J. Xu and Y.-F. Han, *Catal. Sci. Technol.*, 2016, **6**, 5060–5068.
- 45 R. Tu, L. Li, S. Zhang, S. Chen, J. Li and X. Lu, *Catalysts*, 2017, **7**, 175.
- 46 P. Tian, X. Xu, C. Ao, D. Ding, W. Li, R. Si, W. Tu, J. Xu and Y.-F. Han, *ChemSusChem*, 2017, **10**(17), 3342–3346.
- 47 F. Menegazzo, M. Signoretto, M. Manzoli, F. Boccuzzi, G. Cruciani, F. Pinna and G. Strukul, *J. Catal.*, 2009, **268**, 122–130.
- 48 N. M. Wilson, P. Priyadarshini, S. Kunz and D. W. Flaherty, *J. Catal.*, 2018, **357**, 163–175.

